arXiv:cond-mat/0102199v1 [cond-mat.str-el] 12 Feb 2001

A first order phase transition induced by magnetic field and temperature

K. J. Singh, S. Chaudhary, M. K. Chattopadhyay, M. A. Manekar, S. B. Roy and P. Chaddah

Low Temperature Physics Laboratory, Centre for Advanced Technology,

Indore 452013, India

(February 1, 2008)

Abstract

Taking the pseudobinary C15-Laves phase compound $Ce(Fe_{0.96}Al_{0.04})_2$ as a paradigm for studying a ferromagnetic(FM) to antiferromagnetic(AFM) phase transition, we present interesting thermomagnetic history effects in magnetotransport measurements across this FM-AFM transition. We argue that these distinctive hysteretic features can be used to identify the exact nature -first order or second order - of this kind of transition in magnetic systems where electrical transport is strongly correlated with the underlying magnetic order. A comparison is made with the similar FM-AFM transitions observed in Nd and Pr-based manganese compounds with perovskite-type structure.

Typeset using REVTEX

The nature of ferromagnetic (FM) to antiferromagentic (AFM) transition in the perovskite-type manganese oxide compounds $Nd_{1/2}Sr_{1/2}MnO_3$ and $Pr_{1/2}Sr_{1/2}MnO_3$ has been the subject of close scrutiny in recent years [1,2]. The FM-AFM transition observed in these compounds is taken as a sort of a prototype of a first order transition, and certain thermomagnetic features have been highlighted which are thought to be generic of a first order phase transition [1,2]. In the same spirit we have undertaken a study of FM-AFM phase transition in the pseudobinary C15-Laves phase compound $Ce(Fe_{0.96}Al_{0.04})_2$. We find striking thermomagnetic history effects in magnetotransport measurements across the FM-AFM transition in this interesting system.

$CeFe_2$, with its relatively low Curie temperature ($T_C \approx$230K) and reduced magnetic moment ($\approx 2.3\mu_B/f.u.$) [3], is on the verge of a magnetic instability [4]. Neutron measurement has shown the presence of antiferromagnetic fluctuations in the FM ordered state of $CeFe_2$ below 100K [5]. With small but suitable change in electronic structure caused by doping with elements like Co, Al, Ru, Ir, Os and Re at the Fe-site of $CeFe_2$ [6], these antiferromagnetic fluctuations get stabilized into a low temperature AFM state, and after certain concentration of dopants (usually 5 to 10%) this AFM phase replaces the FM phase altogether [7–14].

While most recent experimental efforts are mainly focussed on understanding the cause of this magnetic instability [15,16] in $CeFe_2$, there exists one other aspect of the observed magnetic properties which needs proper attention, viz. the exact nature of the FM-AFM transition. We have recently addressed this second question in Ru and Ir-doped $CeFe_2$ alloys [17,18]. In this paper we shall focus on the Al-doped $CeFe_2$ alloys. In contrast to the Ru, Co and Ir doped alloys, a distinct co-existence of FM and AFM phase has been reported around the FM-AFM transition temperature in Al-doped $CeFe_2$ alloys [12]. We report here interesting thermomagnetic history dependence of magnetotransport in a $Ce(Fe_{0.96}Al_{0.04})_2$ alloy. We argue that these thermomagnetic history effects arise due to the first order nature of the FM-AFM transition. These effects are broader manifestations of the behavior reported earlier in manganese compounds [1], and can be used to identify a first order FM-AFM

transition in a new system, especially in those where the electrical transport is strongly correlated with the underlying magnetic order.

The details of the preparation and characterization of the sample can be found in Ref.10. The samples from the same batch have been used earlier in the study of bulk magnetic and transport properties [10], and neutron measurements [12]. We have used a superconducting magnet and cryostat system (Oxford Instruments, UK) for magnetotransport measurements as a function of temperature (T) and applied magnetic field (H). The resistivity is measured using a standard dc-four probe technique.

The inset of Fig. 1(a) shows the magnetization (M) vs T plot for the $Ce(Fe_{0.96}Al_{0.04})_2$ sample measured with an applied field of 2 mT. The sample undergoes a paramagnetic (PM) to FM transition at around 195K, followed by a lower temperature FM-AFM transition around 90K. These results are in consonance with the earlier bulk properties [10] and neutron measurements [12]. We shall now study the field dependence of magnetoresistance in various temperature regimes. In the main panel of Fig.1 we present resistivity (ρ) as a function of H at T=3K, 5K, 20K, obtained after initial zero-field-cooling (ZFC) the sample to the temperature concerned. The ρ vs H plot at T$\geq$120K (not shown here) is that of a typical ferromagnet, showing clear negative magnetoresistance. In the antiferromagnetic regime (see Fig. 1(a)-(c)), we see the clear signature of a field induced ferromagnetic transition at a field H_M, where the resistivity decreases sharply with the increase in H. (The slight increase in ρ in the field regime H$\leq$$H_M$, indicating the positive magnetoresistance of the AFM state is not quite visible in the same scale). Although the change in resistivity due to this field induced transition is not as drastic as in $Nd_{1/2}Sr_{1/2}MnO_3$ [1], this is within an order of magnitude of those obtained with the similar applied fields in $Pr_{1/2}Sr_{1/2}MnO_3$ [2]. It is to be noted here that the FM-AFM transition in the present sample is not accompanied by a metal-insulator transition and both the FM and AFM states remain metallic. On reducing the field from well above H_M, a distinct hysteresis is observed in the ρ vs H plot (see Fig. 1(a)-(c)). We attribute this to the first order nature of the field induced AFM-FM transition. While reducing H from well inside the FM state i.e. H>> H_M, the FM state continues to exist as

supercooled metastable state below H_M up to a certain metastability field H^* [19]. Between H_M and H^* fluctuations will help in the formation of droplets of the stable AFM state, and at H^* an infinitisimal fluctuation will drive the whole system to the stable AFM state. Similar hysteresis in the ρ-H plots of $Nd_{1/2}Sr_{1/2}MnO_3$ and $Pr_{1/2}Sr_{1/2}MnO_3$ has also been attributed to the first order nature of the phase transition [1,2]. The role of thermal fluctuations is expected to be reduced in the very low temperature regime, and this is clearly seen in the ρ-H plots at T=3K and 5K (see Fig. 1(b) and (c)). In this temperature regime on reduction of the applied H to zero the ρ(H=0) lies distinctly below the intial ZFC-ρ(H=0), thus giving rise to an open hysteresis loop. This kind of open hysteresis loop has earlier been reported for $Nd_{1/2}Sr_{1/2}MnO_3$ [1] but not for $Pr_{1/2}Sr_{1/2}MnO_3$ [2]. We attribute this behaviour to the existence of a residual metastable FM state even when the applied H is reduced to zero. On increasing H on the negative side, the ρ(H) curve is clearly not symmetric to the virgin ρ(H) curve on the positive H side (see Fig. 1(b)-(c)). The field induced AFM-FM transition, however, takes place at the same $|H_M|$ (see Fig. 1(b)-(c)). A distinct hysteresis is observed on reducing H from the same $|H_{max}|$ as in the positive side. The envelope hysteresis loop now closes at H=0, i.e. it merges with the starting value where from the field excursion on the negative direction had started. Further on increasing H to the positive side, the ρ(H) curve now follows a path which is distinctly below the virgin ρ(H) curve but very symmetric to the ρ(H) curve on the negative side in the increasing H cycle. This ρ(H) curve (henceforth will be termed as forward envelope curve) merges with the virgin curve in the H-regime well beyond H_M. We have checked this distinct difference between the virgin curve and the forward envelope curve in the negative H side also, by drawing a virgin curve in the negative H direction after zero field cooling the sample (see dashed line in Fig. 1(b)-(c)). This anomalous behaviour of virgin curve lying distinctly outside the envelope curve is observed [20] in the field dependence of magnetization as well (see inset of Fig. 1(b)).

From a closer inspection of the published results on the $Nd_{1/2}Sr_{1/2}MnO_3$ sample [1], we expect similar behaviour to take place in that sample in the temperature regime T$\leq$20K. Specifically the ρ-H curve was shown to have an open hysteresis-loop (see figs. 2 B to 2D

of ref.1). We expect that if H was reduced to -12T in that sample, and then raised back to +12T, this second leg would be closed similar to our Fig. 1(a). Similarly an isothermal M-H measurement in that compound should show a virgin curve lying outside the envelope curve as in the inset of Fig. 1(b).

Another interesting aspect worth noting in our present sample is that the slope of the ρ(H) return envelope curves change sharply on crossing H=0 in either direction (see Fig. 1(b)-(c)). It almost flattens in the low field regime H< $|H_M|$ on either side of H=0, as if the domains of the residual FM state still retain their previous memory. With the striking similarity of the field dependence of resistivity in $Nd_{1/2}Sr_{1/2}MnO_3$ (see Fig. 2(b)-(d) of Ref.1) with those in the positive H cycle in the present sample (Fig. 1(b)-(c)), it is quite tempting to predict the similar sharp change in slope of R(H), as H changes sign of H in $Nd_{1/2}Sr_{1/2}MnO_3$ as well.

Supercooling/superheating and metastability have been identified as key elements to explain the thermomagnetic history effects associated with the first order FM-AFM transition in perovskite-type manganese oxide systems [1]. To explain the strong temperature dependence of this thermomagnetic irreversibility in our present system, we now invoke in addition the concept of the limit of the metastability H^*(T) (or T^*(H)). The implicit assumption involved here is that the difference between the phase transition line H_M(T) (or T_N(H)) and the limit of metastability H^*(T) (or T^*(H)) widens with the decrease (increase) in temperature (magnetic field). To support this assumption we shall now study the temperature dependence of resistivity in the presence of various applied magnetic fields.

In Fig. 2 we present ρ vs T plots with H=0, 0.5T, 2T and 3T. Appearance of magnetic superzones [10,11] at the FM-AFM transition (T_N) give rise to a distinct structure in the form of a local minimum in the ρ(T) (see Fig.2). There is a marked hysteresis associated with this transition, emphasizing the first order nature of the transition. We argue that the FM (AFM) phase exists as supercooled (superheated) metastable phase in the cooling (heating) cycle in this hysteretic temperature regime. In the high (low) temperature reversible regime the only magnetic phase is the stable FM (AFM) phase. In an earlier zero field

neutron measurement [12] a clear co-existence of FM-AFM phase was observed for a substantial temperature regime below the onset of phase transtion. This alongwith the gradual development of the cubic to rhombohedral structual distortion [12] as the temperature is lowered, fit naturally in our present picture of first order phase transition. In the presence of finite H [21] the T_N is suppressed and the hysteresis is enhanced substantially, so much so that with H=2T no reversible regime is observed below T_N down to 5K. This in turn implies that the limit of metastability $T^*(H)$ (below which one should see the reversible response of the stable AFM phase) gets suppressed even faster in comparison to $T_N(H)$, and the metastable regime (encompassed between $T_N(H)$ and $T^*(H)$) widens with the decrease in T or with increase in H. This is again in perfect consonance with our observation in the isothermal field dependence of resistivity.

Summarizing our results, the important findings of the present study are the following:

1. The butterfly ρ(H) hysteresis loop with anomalous virgin curve, which does not close at H=0 in the low temperature regime. This is complimented with magnetization study as well.

2. The distinct hysteresis in the ρ(T) curve at AFM-FM transition, which gets enhanced in the presence of applied magnetic field.

These observations along with the earlier neutron measurements [12] help to establish the first order nature of the AFM-FM transition in the $CeFe_2$-based pseudobinary systems. This information in turn will be important for developing a theoretical model to explain the interesting electro-magnetic properties of $CeFe_2$, which does not exist so far. Most importantly, thermomagnetic history effects observed here can be used as generic features to identify a first order FM-AFM phase transition. In fact the double hysteresis or butterfly loop in polarization measurements is regularly used to identify a first order transition in the ferroelectric/antiferroelectric materials [22]. (However, we are unaware of any report regarding the anomalous nature of the virgin curve associated with the butterfly loops in the ferroelectric materials). Such a field induced first order transition can be explained in terms of free en-

ergy curves obtained by expanding in a power series in polarization and retaining only terms with even powers up to sixth order [22]. Phase coexistence and metastability across the first order phase transition, and hence hysteresis arise naturally out of such free energy curves. Although, sharp rise in field induced magnetization (and associated hysteresis) [13] and sharp drop in the field induced resistivity [14,23] in magnetic systems are regularly taken as signatures of AFM-FM transition, no clearcut inference can be made from such observations regarding the exact nature of the phase transition. Our present study along with those on perovskite-type manganese oxide systems [1,2] attempt to fill-up this gap and provide some relatively easy means to identify the nature of such magnetic transitions from standard bulk properties measurements. It should be noted here that the resistivity/magnetoresistance is not a thermodynamic quantity, whereas magnetization/staggered magnetization is, and can be used as an order parameter in the Landau type free energy expansion. However, intricate correlation between the resistivity/magnetoresistance and magnetization/staggered magnetization across the FM-AFM transition, makes these magnetotransport properties suitable observables in the study of the nature of the phase transition. Further, these samples with well characterized electro-magnetic properties can be used as paradigms to study the various interesting aspects of a first order transition, namely nucleation and growth, and path dependence of the transition, in a relatively easy and reproducible manner. Such studies are not that easy and reproducible in the more common cases of first order transition, like melting (solidification) of solids (liquids) or vaporization (condensation) of liquids (gases).

REFERENCES

[1] KUWAHARA H., et al, Science, **270** (1995) 961.

[2] TOMIOKA Y., et al, Phys. Rev. Lett. **74** (1995) 5108.

[3] ERIKSSON O., NORDSTROM L., BROOKS M. S. S. and JOHANSSON B., Phys. Rev. Lett. **60** (1988) 2523.

[4] ROY S. B. and COLES B. R., J. Phys. F:Met. Phys. **17** (1987) L215.

[5] PAOLASINI L et al, Phys. Rev. **B58** (1998) 12117.

[6] KHOWASH P. K., Phys. Rev. **B43** (1991) 6170.

[7] FRANCESCHINI D. F. and Da CUNHA S. F., J. Magn. Magn. Matter. **52** (1985) 280.

[8] RASTOGI A. K. and MURANI A. P., in Theoretical and Experimental Aspects of Valence Fluctuations and Heavy Fermions, edited by L. C. Gupta and S. K. Malik (New York: Plenum, 1987) p437.

[9] PILLAY R. G. et al, J. Phys. F:Met. Phys. **18** (1988) L63 .

[10] ROY S. B. and COLES B. R., J. Phys.: Condens. Matter. **1** (1989) 419.

[11] ROY S. B. and COLES B. R., Phys. Rev. **B39** (1989) 9360.

[12] KENNEDY S. J. and COLES B. R., J. Phys.: Condens. Matter, **2** (1990) 1213.

[13] ALI N. and Zhang X., J. Phys.: Condens. Matter. **4** (1992) L351.

[14] NIGAM A. K., RADHA S., ROY S. B. and CHANDRA G., Physica **B205** (1995) 421.

[15] CHABOY J et al, Phys. Rev. **B62** (2000) 468.

[16] LANGE R. J., et al, Phys. Rev. **B62** (2000) 7084.

[17] MANEKAR M. A., ROY S. B. and CHADDAH P, J. Phys.:Condens. Matter. **12** (2000) L409 .

[18] MANEKAR M et al, J. Phys.:Condens. Matter **12** (2000) 9645.

[19] CHAIKIN P. M. and LUBENSKY T. C., Principles of Condensed Matter Physics (Cambridge University Press, 1995).

[20] MANEKAR M. A. et al, cond-mat/0012472.

[21] In the resistivity measurements in presence of finite H, we first zero-field cool the sample to the lowest temperature of measurement, switch on the field, warm up the sample to the highest temperature of measurement, and then cool back the sample (in presence of the field) across the phase transition temperature down to the lowest temperature of measurement.

[22] A. J. Dekker, Solid State Physics (Macmillan India Ltd., 1985).

[23] KUNKEL H. P., et al, Phys. Rev. **B53** (1996) 15099.

FIGURES

FIG. 1. Resistivity vs field plots of $Ce(Fe_{0.96}Al_{0.04})_2$ at T=20K, 5K and 3K. The open square symbols represent the envelope curves initiated between the respective $\pm\mu_0 H_{max}$ as indicated in the figures. Closed squares show the "virgin" curve where the sample is cooled in zero field and the field is then raised to 10T. Inset of Fig. 1(a) shows the magnetization vs temperature plot obtained with a field of 2 mT. Inset of Fig. 1(b) shows the magnetization vs field plot at T=5K. The virgin (envelope) curve is shown by filled (open) triangle symbols; note that the virgin curve is lying outside the envelope curve.

FIG. 2. Resistivity (ρ) vs temperature plots in the presence of various applied fields H=0, 0.5T, 2T and 3T shown by square, triangle, circle and diamond symbols respectively. The experimental protocol is described in Ref.21. The open (filled) symbols show the ρ(H)-T behaviour of the sample recorded during warming (cooling). Inset shows the zero field ρ-T plot showing both the PM-FM and FM-AFM transitions.

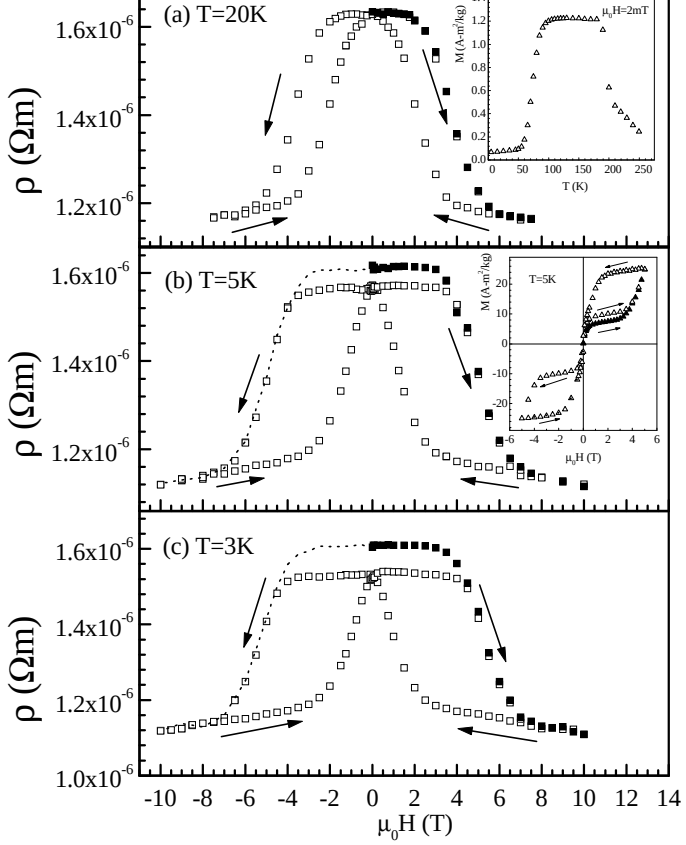
(a) T=20K
(b) T=5K
(c) T=3K
ρ (Ωm)
1.6x10-6
1.4x10-6
1.2x10-6
1.0x10-6
-10 -8 -6 -4 -2 0 2 4 6 8 10 12 14
μ0H (T)
M (A-m2/kg)
μ0H=2mT
T (K)
T=5K
μ0H (T)

Fig. 1 of 2

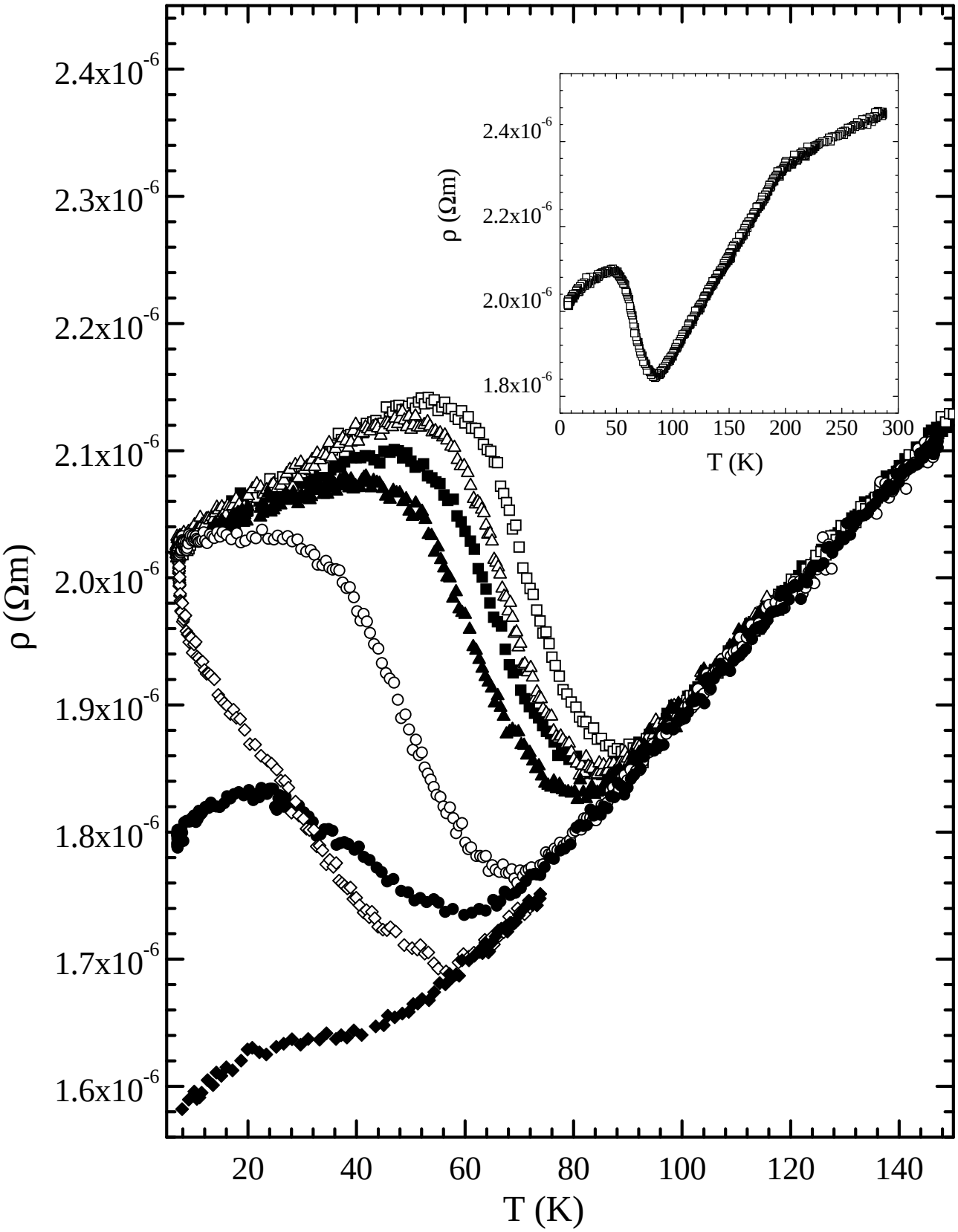
ρ (Ωm)
T (K)
2.4x10-6
2.3x10-6
2.2x10-6
2.1x10-6
2.0x10-6
1.9x10-6
1.8x10-6
1.7x10-6
1.6x10-6
20
40
60
80
100
120
140
ρ (Ωm)
T (K)
2.4x10-6
2.2x10-6
2.0x10-6
1.8x10-6
0
50
100
150
200
250
300

Fig. 2 of 2